Flowfield Simulation and Performance Measurement of Electrothermal Pulsed Plasma Thrusters onboard Osaka Institute of Technology PROITERES Nano-Satellite Series

IEPC-2013-99

Presented at the 33rd International Electric Propulsion Conference,
The George Washington University • Washington, D.C. • USA
October 6 – 10, 2013

Masato Tanaka[1], Rikio Muraoka[2], Shuya Kisaki[3], Chen Huanjun[4], Hirokazu Tahara[5]
Osaka Institute of Technology
*5-16-1, Omiya, Asahi-Ku, Osaka 535*8585, Japan*

and

Takashi Wakizono[6]
High Serve
780-7, Tomehara, Akiruno, Tokyo 190-0152, Japan

Abstract: The Project of Osaka Institute of Technology Electric-Rocket-Engine onboard Small Space Ship (PROITERES) was started at Osaka Institute of Technology in 2007. In PROITERES, a nano-satellite with electrothermal pulsed plasma thrusters (PPTs) was successfully launched on September 9th, 2012 by Indian PSLV launcher C-21. The main mission is powered flight of small/nano satellite by electric thruster. The PPT performance in the 1st PROITERES reached 5.0 Ns with no miss-firing in ground experiments. An unsteady numerical simulation was carried out to investigate physical phenomena in the PPT discharge system including plasma and discharge electric circuit and to predict performance characteristics for small/nano satellites like PROITERES satellites. The calculated Mach number intensively increased downstream from the discharge cavity exit; that is, the supersonic flow was established in the nozzle cathode. Both the calculated impulse bit and mass shot agreed well with the measured ones. The calculated results of 40,000-shot endurance test also agreed with the measured ones. Furthermore, the research and development of the 2nd PROITERES satellite with high-power and large-total-impulse PPT system are introduced.

Nomenclature

C	=	electric capacitance
e	=	internal energy or electron charge
E_i	=	corresponding voltage of ionization
j	=	current density
J	=	discharge current

[1] Graduate Student, Graduate School Major in Mechanical Engineering, and tahara@med.oit.ac.jp.
[2] Graduate Student, Graduate School Major in Mechanical Engineering, and tahara@med.oit.ac.jp.
[3] Graduate Student, Graduate School Major in Mechanical Engineering, and tahara@med.oit.ac.jp.
[4] Graduate Student, Graduate School Major in Mechanical Engineering, and tahara@med.oit.ac.jp.
[5] Professor, Department of Mechanical Engineering, and tahara@med.oit.ac.jp.
[6] Researcher, Electric Propulsion R&D Section, and tahara@med.oit.ac.jp.

k = Boltzmann factor or heat conductivity
L = electric inductance
m = particle mass
M = momentum flux
n = number density
p = pressure
q = heat flux
Q = electric charge
Q_j = Joule heat
r = radial coordinate
R = electric resistance
t = time
T = number density
V = velocity
z = axial coordinate
α = degree of ionization
φ = particle number flux
ρ = density
ρ_p = electric resistance
$\sigma_{e\text{-}n}$ = cross-section of electron-neutral collision
Γ = mass flux
Θ = temperature
0 = initial
e = electron
i = ion
n = neutral
r = radial direction
s = surface
z = axial direction

I. Introduction

THE Project of Osaka Institute of Technology Electric-Rocket-Engine onboard Small Space Ship (PROITERES) was started at Osaka Institute of Technology (OIT) in 2007.[1-13] In PROITERES, a nano-satellite with electrothermal pulsed plasma thrusters (PPTs) was successfully launched by the Indian PSLV C-21 launcher on September 9th, 2012. The main mission is to achieve powered flight of a nano-satellite by an electric thruster and to observe Kansai district in Japan with a high-resolution camera. Figure 1 and Table 1 show the specification and photo, respectively, of the flight model (FM) and launching of the PROITERES satellite. Just now, the PROITERES satellite is under operation; that is, the special FM command of PPT firing is transmitted to the satellite from the ground station at OIT.

Pulsed plasma thrusters are expected to be used as a thruster for small/nano satellites.[14-31] The PPT has some features superior to other kinds of electric propulsion. It has no sealing part, simple structure and high reliability, which are benefits of using a solid propellant, mainly Teflon® (poly-tetrafluoroethylene: PTFE). At Osaka Institute of Technology, the PPT has been studied since 2003 in order to understand physical phenomena and improve thrust performances with both experiments and numerical simulations. We mainly studied electrothermal-acceleration-type PPTs, which generally had higher thrust-to-power ratios (impulse bit per unit initial energy stored in capacitors) and higher thrust efficiencies than electromagnetic-acceleration-type PPTs. Although the electrothermal PPT has lower specific impulse than the electromagnetic PPT, the low specific impulse is not a significant problem as long as the PPT uses solid propellant, because there is no tank nor valve for liquid or gas propellant which would be a large weight proportion of a thruster system.

At OIT, the project of 2nd PROITERES, as shown in Fig. 2 and Table 2 was started in 2010. The 2nd PROITERES satellite aims at powered flight with longer distance, i.e. changing 200-400 km in altitude on near-earth orbits, than that of the 1st PROITERES. We are developing high-power and high-total-impulse PPT systems, in which conceptual designs of PPT system and initial performances are investigated for high-power and high-total-impulse operations. In this paper, we introduce numerical simulation project to predict performance of PPT systems for PROITERES satellite series at OIT.[25-31]

Table 1. Specification of 1st PROITERES Satellite.

Specifications	Value
Mass	14.5kg
Dimensions	Cube, 300mm on a side
Electrical power	10W
Altitude	670km
Development period	4year
Life time	More than one year
Orbit	Sun-synchronous orbit
Launch vehicle	PSLV

Fig. 1. Photos of 1st PROITERES satellite FM and launching.

Table 2. Specification of 2nd PROITERES satellite.

Specifications	Value
Mass	50kg
Dimensions	Cube, 500mm on a side
Electrical power	62W
Development period	3year
Life time	More than one year
Launching due date	The second half of 2014
Main missions	Long-distance power flight

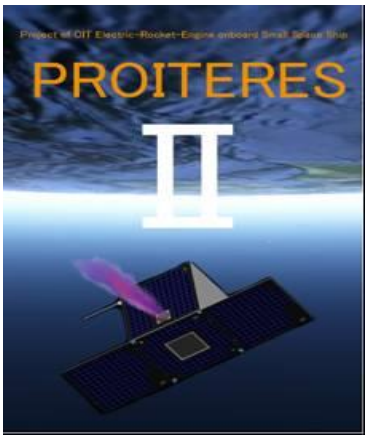

Fig. 2. Illustration of2nd PROITERES satellite.

II. Thrust Measurement System

Figure 3 shows a thrust stand in a vacuum chamber for precise measurement of an impulse bit.[14-21] The PPT and capacitors are mounted on the pendulum, which rotates around fulcrums of two knife edges without friction. The displacement of the pendulum is detected by an eddy-current-type gap sensor (non-contacting micro-displacement meter) near the PPT, which resolution is about ± 0.5 μm. The electromagnetic damper is used to suppress mechanical noises and to decrease quickly the amplitude for the next measurement after firing the PPT. It is useful for a sensitive thrust stand because it is non-contacting. The damper consists of a permanent magnet fixed to the pendulum and two coils fixed to the supporting stand. The control circuit differentiates the output voltage of the displacement sensor and supplies the current proportional to the differentiated voltage to the coil. Accordingly, the damper works as a viscosity resistor. The damper is turned off just before firing the PPT for measurements without damping, and turned on after the measurement to prepare for the next measurement. Figure 4 shows a typical signal of displacement in measurement of impulse bit. Sensitiveness of the thrust stand is variable by changing the weight mounted on the top of the pendulum as shown in Fig. 5. A calibration of the thrust stand is carried out by collisions of balls to the pendulum with various balls from various distances corresponding to 15-1400 μNs.

Figure 6 shows a vacuum chamber 1.25 m in length and 0.6 m in inner diameter, which is evacuated using a turbo-molecular pump with a pumping speed of 3,000 l/s. The pressure is kept below 1.0×10^{-2} Pa during PPT operation.

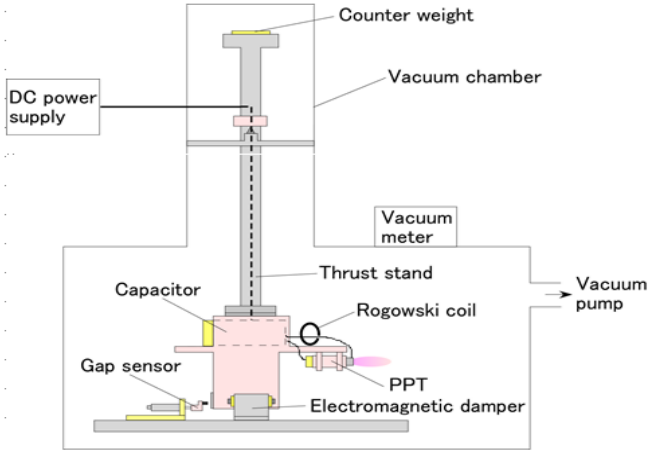

Fig. 3. PPT experimental system.

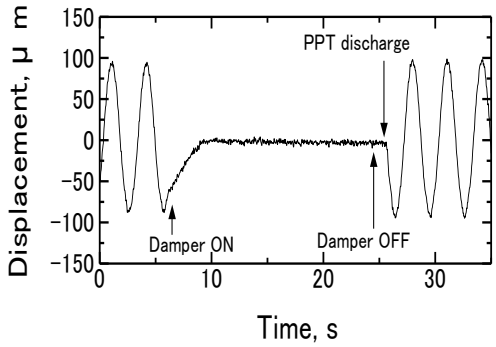

Fig. 4. Typical signal of displacement in measurement of impulse bit.

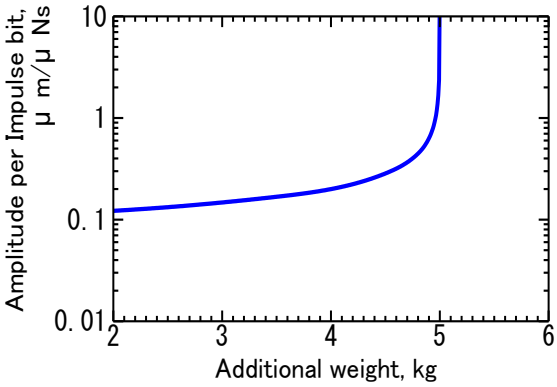

Fig. 5. Sensitiveness of thrust stand vs top weight.

Fig. 6. PPT experimental system installed in vacuum chamber

III. Numerical Calculation

A. Calculation model

An unsteady numerical simulation is carried out to investigate physical phenomena in the PPT discharge system including plasma and discharge electric circuit and to predict performance characteristics.[22-31] Figure 7 shows the calculation model of the PPT system. The calculation simultaneously simulates unsteady phenomena of discharge in the circuit, heat transfer to the PTFE, heat conduction inside the PTFE, ablation from the PTFE surface and plasma flow. The calculation domain of the discharge chamber, as shown in Fig. 8, in the nozzle cathode and in the cylindrical cavity made of PTFE (Teflon). The length and diameter of the cavity are changed considering operational conditions.

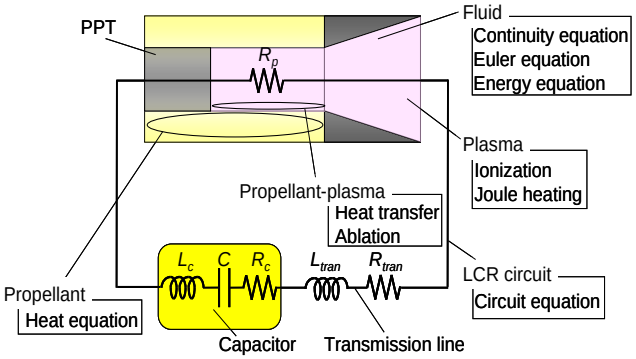

Fig. 7. Calculation model for PPT system.

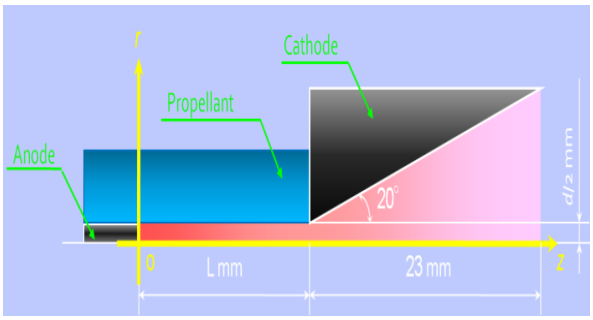

Fig. 8. Calculation domain.

B. Governing equations

The axisymmetric two-dimensional unsteady flowfield equations, conservation equations of mass, momentum and energy, are written as follows:

Mass:

$$\frac{\partial}{\partial t}\rho+\frac{\partial}{\partial r}M_r+\frac{\partial}{\partial z}M_z=-\frac{1}{r}M_r \tag{1}$$

Momentum (Euler Eqs.):

r-direction:

$$\frac{\partial}{\partial t}M_r+\frac{\partial}{\partial r}\left[\frac{M_r^{\,2}}{\rho}+p\right]+\frac{\partial}{\partial z}\left[\frac{M_rM_z}{\rho}\right]=-\frac{1}{r}\frac{M_r^{\,2}}{\rho} \tag{2}$$

z-direction:

$$\frac{\partial}{\partial t}M_z+\frac{\partial}{\partial r}\left[\frac{M_rM_z}{\rho}\right]+\frac{\partial}{\partial z}\left[\frac{M_z^{\,2}}{\rho}+p\right]=-\frac{1}{r}\frac{M_rM_z}{\rho} \tag{3}$$

Energy:

$$\frac{\partial}{\partial t}e+\frac{\partial}{\partial r}\left[\frac{M_r}{\rho}(e+p)\right]+\frac{\partial}{\partial z}\left[\frac{M_z}{\rho}(e+p)\right]=-\frac{1}{r}\frac{M_r}{\rho}(e+p)+Q_j \tag{4}$$

where ρ, p, and e are density, pressure and internal energy of flow, respectively, and M_r and M_z are momentum fluxes of raidial and axial directions, respectively. Q_j is Joule heat.

Ionization equilibrium is assumed as follows:

Saha Eq.:

$$\frac{\alpha^2}{1-\alpha^2}=2.6\frac{(kT)^{5/2}(2\pi m_e)^{3/2}}{p\,h^3}\exp\left(-\frac{qE_i}{kT}\right) \tag{5}$$

where α and T are degree of ionization and temperature of flow, respectively, and E_i is corresponding voltage of ionization, in which the average ionization voltage of PTFE decomposed atoms (carbon and hydrogen etc.) are used.

The Joule heat is written as follows:

$$Q_j=\rho_p\,j^2 \tag{6}$$

$$\rho_p=\frac{\ln\Lambda}{1.53\times10^{-2}T^{3/2}}+\frac{m_e}{n_e e^2}\cdot\sigma_{e-n}n_n\left(\frac{3kT}{m_e}\right)^{1/2}$$

$$\ln\Lambda=\ln[12\pi n_e(\varepsilon_0 kT/e^2n_e)^{3/2}]$$

where ρ_p is electric resistance corresponding electron-ion and electron-neutral collisions, in which n_e and n_n are densities of electron and neutral, respectively, and j is current density in axial direction.

Figure 9 shows the model of heat fluxes from plasma to PTFE surface in the cavity, and their heat fluxes and the interaction are written as follows:

Heat convection:

$$q_{h,conv} = a_i(\varphi_i + \varphi_n)\cdot 2k(T_{h,w} - T_s) \tag{7}$$

Heat conduction:

$$q_{h,cond} = k\frac{\partial T_{h,w}}{\partial r} \tag{8}$$

Interaction Eq.:

$$q_{h,conv} = q_{h,cond} \tag{9}$$

where φ_i and φ_n are particle number fluxes of ion and neutral, respectively, to PTFE surface.

In evaporation of PTFE on the cavity wall, we uses the following equations:

Langmuir's law:

$$\Gamma = \left(\frac{m_n}{2\pi kT_s}\right)^{1/2} p_{vap} \tag{10}$$

($p_{vap} = p_c \exp(-T_c / T_s)$
$p_c = 1.84 \times 1015$ Pa、$T_c = 20815$ K)

Evaporation heat flux:

$$q_{ab} = \frac{\Gamma}{m_n}\cdot 2kT_s \tag{11}$$

where Γ and q_{ab} are mass and heat fluxes, respectively, from PTFE surface, and p_{va} and T_s are evaporation pressure and PTFE surface temperature, respectively.

In heat conduction inside the PTFE block, the heat conduction equation and the boundary condition are written as follows:

$$\frac{\partial \Theta}{\partial t} = \frac{\kappa}{\rho_{PTFE} C_p}\left(\frac{\partial^2 \Theta}{\partial r'^2} + \frac{1}{r'}\frac{\partial \Theta}{\partial r'} + \frac{\partial^2 \Theta}{\partial z^2}\right) \tag{12}$$

$$\kappa \left.\frac{\partial \Theta}{\partial r}\right|_{r=0} = (Q_{conv} - Q_{ab})$$

where Θ is temperature inside the PTFE.

Finally, we close the equation system by using the following electric circuit equation:

From Fig. 7:

$$(L_{tran} + L_c)\ddot{Q} + (R_{tran} + R_c + R_p)\dot{Q} + \frac{Q}{C} = 0 \tag{13}$$

$$J = -\dot{Q}$$

Initial condition:

$$Q_0 = CV_0$$

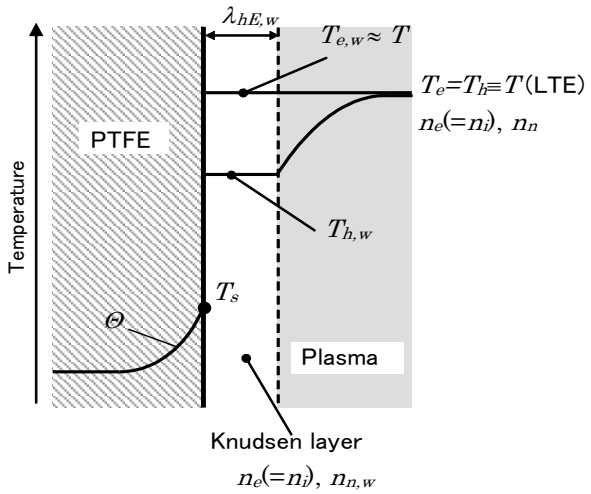

Fig. 9. Heat transfer inside PTFE.

C. Calculation procedure and conditions

After all equations were normalized, the flowfield equations are numerically solved by TVD-MacCormack scheme and average of Roe. In the calculation process, the electric circuit equation is solved by Runge-Kutta method, and the axial current density is obtained. The boundary conditions shown in Fig. 10 are assumed. For calculation start, a very low density plasma is distributed just before the calculation. The calculation grid sizes are 0.5 mm in axial direction and 0.025 mm in radial direction, and the time step is 10^{-9} s.

The experimental and calculation conditions are shown in Tables 3-5. The discharge energies per one shot are 14.6 and 2.4 J/shot; that is, the capacitance is changed. Accordingly, the length and diameter of discharge cavity are changed to find preferable cavity configuration. The discharge energy per one shot is lowered to 2.4 J/shot for the nano satellite.

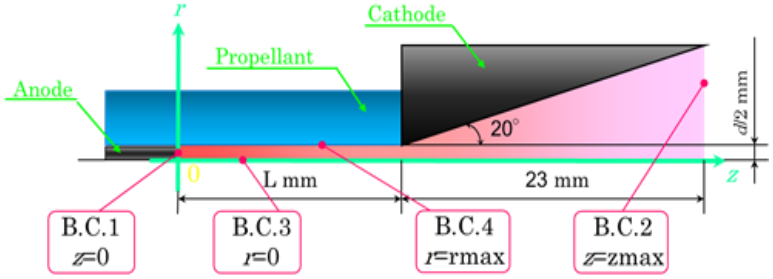

	ρ	M_r	M_z	e
B.C 1	$\frac{\partial \rho}{\partial z} = 0$	$\frac{\partial M_r}{\partial z} = 0$	$M_z = 0$	$\frac{\partial e}{\partial z} = 0$
B.C 2	$\frac{\partial \rho}{\partial z} = 0$	$\frac{\partial M_r}{\partial z} = 0$	$\frac{\partial M_z}{\partial z} = 0$	$\frac{\partial e}{\partial z} = 0$
B.C 3	$\frac{\partial \rho}{\partial r} = 0$	$M_r = 0$	$\frac{\partial M_z}{\partial r} = 0$	$\frac{\partial e}{\partial r} = 0$
B.C 4	$\Delta\rho_r = \rho_{ab}$	$M_r = \Gamma$	$\frac{\partial M_z}{\partial r} = 0$	$\Delta e_r = Q_{ab} - Q_{conv}$

Fig. 10. Boundary conditions.

Table 3. Experimental and calculating condition with discharge energy per one shot of 14.6 J/s.

Discharge chamber	Length, mm	19
	Diameter, mm	2.5, 3.0, 3.5
Nozzle	Length, mm	23
	Half angle, degree	20
Charging voltage, V		1800
Capacitance, μF		9.0

Table 4. Experimental and calculating condition with discharge energy per one shot of 2.4 J/s.

Discharge chamber	Length, mm	9.0
	Diameter, mm	1.0, 1.5, 2.0, 2.5
Nozzle	Length, mm	23
	Half angle, degree	20
Charging voltage, V		1800
Capacitance, μF		1.5

Table 5. Experimental and calculating condition of endurance test.

Discharge chamber	Length, mm	10.0
	Diameter, mm	1.0
Nozzle	Length, mm	23
	Half angle, degree	20
Capacitance, μF		1.5
Charging voltage, V		1800
Inductance, μH		0.35
Resistance, Ω		0.05

IV. Results and Discussion

A. Physical feature in discharge chamber

Figure 11 shows typical measured and calculated discharge current signals with a discharge energy of 14.6 J/s. The calculated current signal agrees with the measured one.

Figure 12 shows the calculated Mach number distribution just after 3 μs from the discharge start with 14.6 J/s. The Mach number intensively increases downstream from z=19mm; that is, the supersonic flow is established. At z=35mm, the Mach number drastically decreases downstream, resulting from structure of shock wave.

Figure 13 shows the calculated time histories of normalized density, thrust, ablated mass and Joule heating at r=1.25mm and z=9.5mm with 14.6 J/s. The Joule heating begins at approximately 1 μs; it is completed by 7 μs, and the ablation from the PTFE surface relays about 1-2 μs from the Joule heating. The density gradually increases from about 2 μs; it has a peak at 9 μs, and then it decreases. The thrust gradually increases from 4 μs, and it has a peak at 13 μs. Accordingly, The thrust is generated until over 20 μs. Thrust generation is expected to be related to increase in density.

Figure 14 shows axial the calculated distributions of normalized density, velocity and ablation flux near the cavity wall just after 10 μs from the discharge start with 14.6 J/s. The velocity linearly increases from the upstream end to the cavity exit although the density gradually decreases. An axial decrease in ablation flux is due to the axial decrease in density because of lowering heat convection to the PTFE surface.

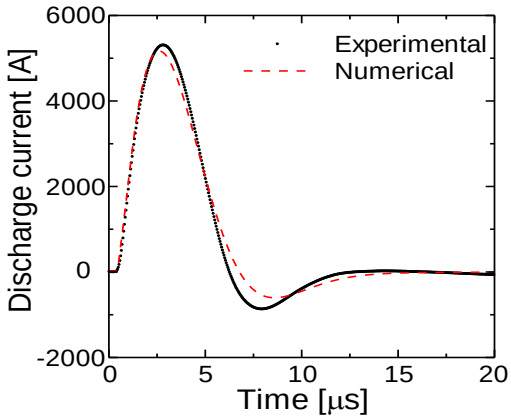

Fig. 11. Discharge current signal.

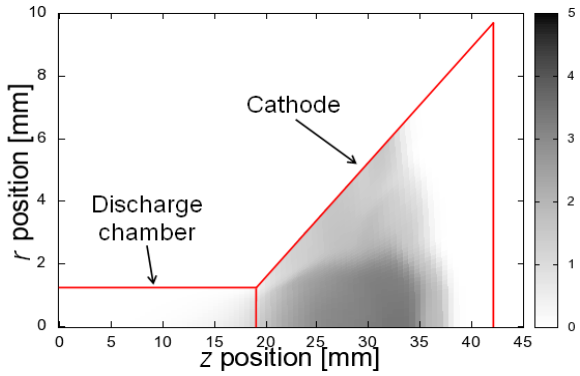

Fig. 12. Mach number distribution.

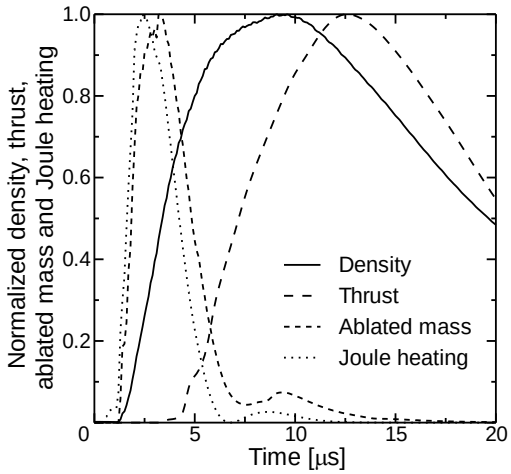

Fig. 13. Normalized density, thrust, Joule heating and ablated mass.

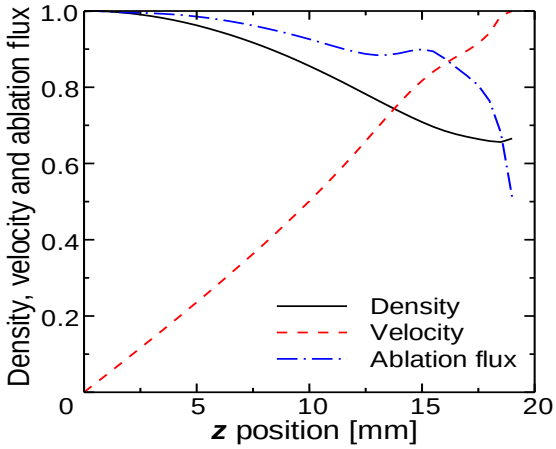

Fig. 14. Normalized density, velocity and ablation flux.

B. Comparisons with experimental results

Figure 15 shows measured and calculated impulse bit and mass shot dependent on cavity diameter with a constant cavity length of 19 mm with a discharge energy per one shot of 14.6 J/s. Both the impulse bit and the mass shot decrease with increasing cavity diameter regardless of calculation and experiment. The calculated impulse bit roughly agrees with the measured one although with a small diameter of 2.5 mm it is slightly higher. On the other hand, the calculated mass shot agrees with the measured one, and its error is within 10 % although it is lower with all cavity diameters.

Figure 16 shows measured and calculated impulse bit and mass shot dependent on cavity diameter with a constant cavity length of 9 mm with a discharge energy per one shot of 2.4 J/s. Both the calculated impulse bit and mass shot agreed with the measured ones even with low discharge energies.

C. Calculated endurance test results

We simply calculated repetitive operation modes, i.e., endurance tests of the PPT system by using a one-dimensional model with the same assumptions of the axisymmetric model. Figure 17 shows the calculated results. Both the impulse bit and the mass shot have the maximum errors of 25 % compared with the measured ones in the range up to 20,000 shots. However, they agree well with the measured ones in the long operation above 20,000 shots.

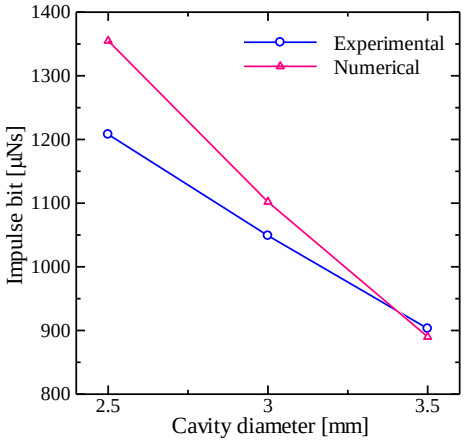

(a)

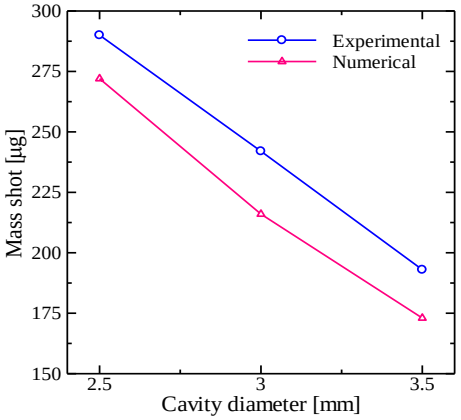

(b)

Fig. 15. Experimental and numerical results with discharge energy per one shot of 14.6 J/s. a) Impulse bit; b) Mass shot.

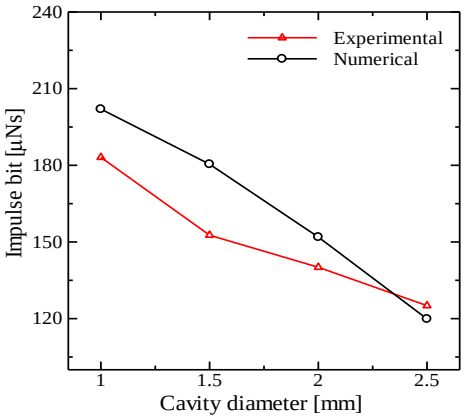

(a)

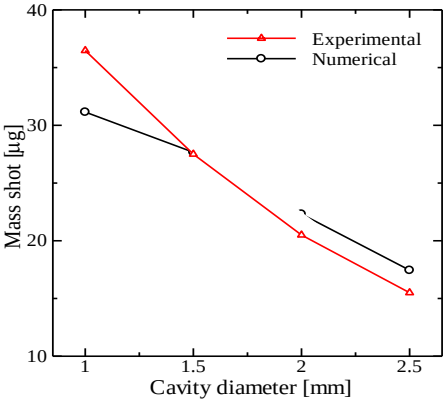

(b)

Fig. 16. Experimental and numerical results with discharge energy per one shot of 2.4 J/s. a) Impulse bit; b) Mass shot.

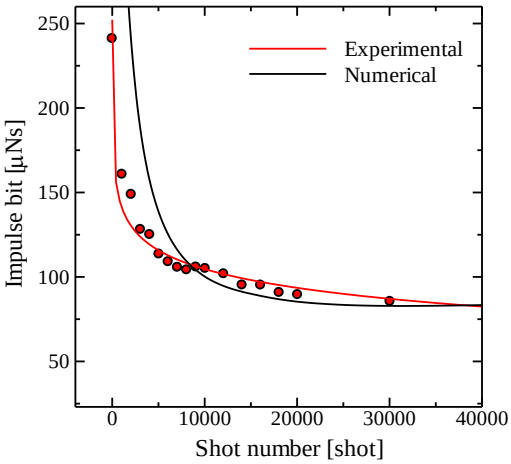

(a)

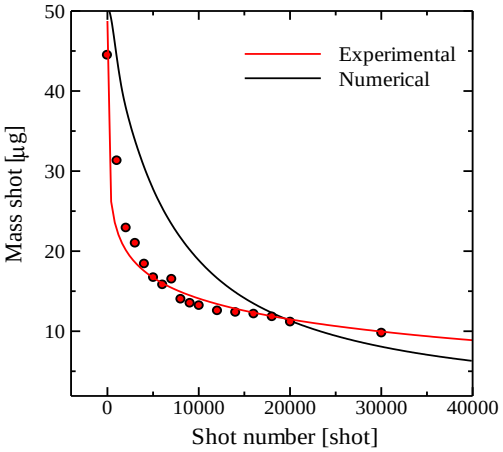

(b)

Fig. 17. Experimental and numerical results of endurance test with 2.4 J/s. a) Impulse bit; b) Mass shot.

V. PPT Performance Prediction for 2nd PROITERES Satellite

The charging energy is changed from 2.4 J/s for the 1st PROITERES satellite to 31.6 J/s for the 2nd PROITERES one.

D. Cavity length dependence

The calculation was carried out for single shot (initial condition) and 400 shots with a constant cavity diameter of 5 mm and changing lengths of 10-25 mm. As shown in Figs. 18 and 19, both the impulse bit and the mass shot increase with cavity length. The performance with single initial shot is higher than that after 400 shots. The maximum impulse bit of about 1.5 Ns was predicted with a cavity length of 25 mm.

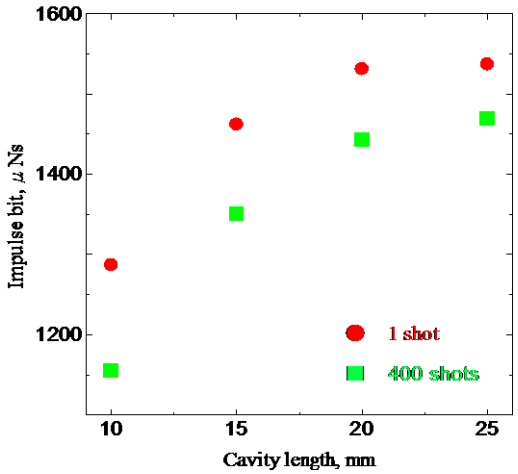

Fig. 18. Cavity length dependence of impulse bit.

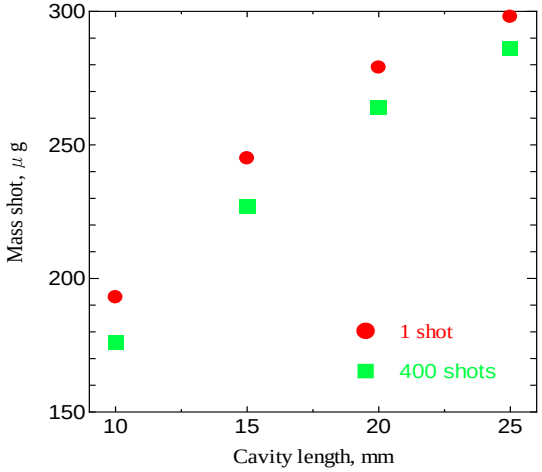

Fig. 19. Cavity length dependence of mass shot.

E. Cavity diameter dependence

With a cavity length of 10 mm, the cavity diameter was changed from 2.4 to 5 mm. As shown in Figs. 20 and 21, both the impulse bit and the mass loss linearly decrease with increasing cavity diameter. This is expected because of decreasing pressure in the cavity when increasing cavity diameter. Of course, the performance with single initial shot is higher than that after 400 shots. The maximum impulse bit around 2 Ns was predicted with a cavity diameter of 2.4 mm.

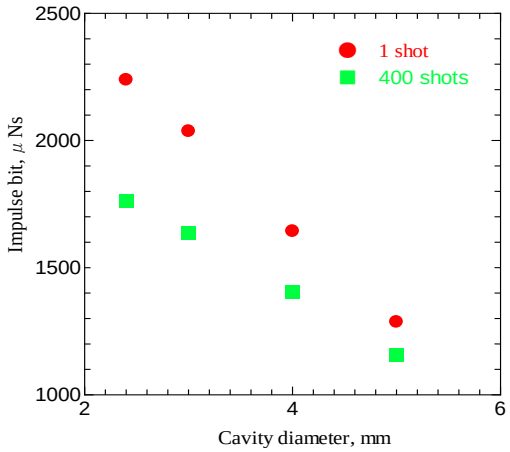

Fig. 20. Cavity diameter dependence of impulse bit.

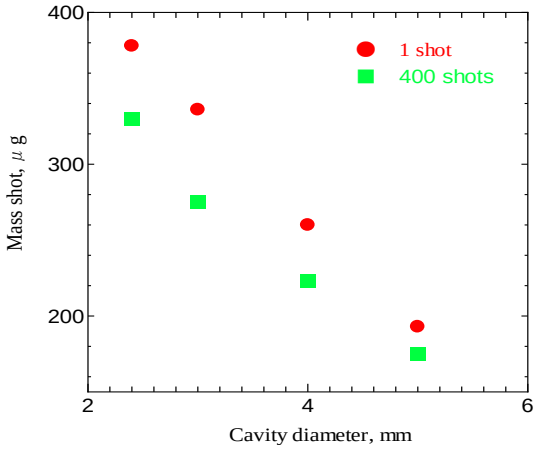

Fig. 21. Cavity diameter dependence of Mass shot.

F. 10000shot endurance test performance

In calculation for endurance, the cavity length and diameter were set to 25 mm and 5 mm, respectively, with a constant charging energy of 31.59 J/shot. The calculation result of 10000 shots is shown in Fig. 22. Both the impulse bit and mass consumption decreases with increasing shot number. This is expected because the cavity diameter becomes larger with increasing shot number.

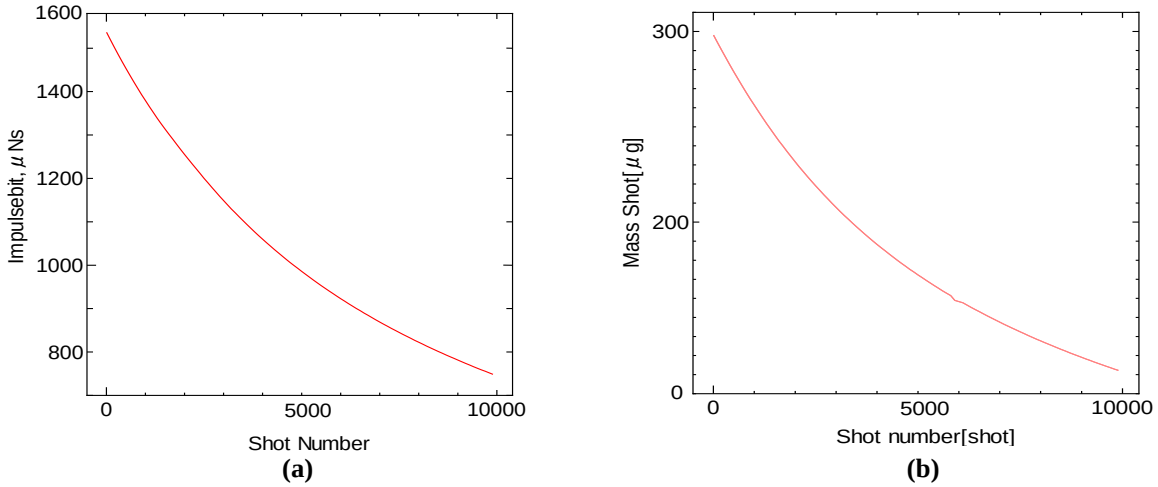

Fig. 22. Numerical results of endurance test with 31.59 J/s. a) Impulse bit; b) Mass shot.

VI. Summary

The Project of Osaka Institute of Technology Electric-Rocket-Engine onboard Small Space Ship (PROITERES) was started at Osaka Institute of Technology in 2007. In PROITERES, a nano-satellite with electrothermal pulsed plasma thrusters (PPTs) was launched on September 9th, 2012 by Indian PSLV launcher C-21. The main mission is powered flight of small/nano satellite by electric thruster. The PPT performance in 1st PROITERES reached 5.0 Ns with no miss-firing. An unsteady numerical simulation was carried out to investigate physical phenomena in the PPT discharge system including plasma and discharge electric circuit and to predict performance characteristics for small/nano satellites like PROITERES satellites. The calculated Mach number intensively increased downstream from the discharge cavity exit; that is, the supersonic flow was established in the nozzle cathode. Both the calculated impulse bit and mass shot agreed well with the measured ones. The calculated results of 40,000-shot endurance test also agreed with the measured ones. Furthermore, the research and development of the 2nd PROITERES satellite with high-power and large-total-impulse PPT system were investigated. The performance was predicted with changing cavity length and diameter, and the endurance test was also calculated. The maximum impulse bit of 1-2.5 Ns was predicted.

References

[1] Ikeda, T., Yamada, M., Shimizu, M., Fujiwara, T., Tahara, H. and Satellite R&D Team of Students and Faculty Members of OIT," Research and Development of an Attitude Control System for Osaka Institute of Technology Electric-Rocket-Engine onboard Small Space Ship," 27th International Symposium on Space Technology and Science, Tsukuba, Japan, 2009, Paper No. ISTS 2009-s-02f.

[2] Yamada, M., Ikeda, T., Shimizu, M., Fujiwara, T., Tahara, H. and Satellite R&D Team of Students and Faculty Members of OIT," Progress of Project of Osaka Institute of Technology Electric-Rocket-Engine onboard Small Space Ship," 27th International Symposium on Space Technology and Science, Tsukuba, Japan, 2009, Paper No. ISTS 2009-s-05f.

[3] Yamada, M., Ikeda, T., Fujiwara, T. and Tahara, H.," Project of Osaka Institute of Technology Electric-Rocket-Engine onboard Small Space Ship," 31st International Electric Propulsion Conference, University of Michigan, Ann Arbor, Michigan, USA, 2009, Paper No. IEPC-2009-051.

[4] Araki, S., Ikeda, T., Ozaki, J., Nishizawa, M,. Inoue, Y., Iguchi, T. and Tahara, H.," Development of an Attitude Control System for Nano-Satellite PROITERES," 28th International Symposium on Space Technology and Science, Okinawa Convention Center, Ginowan-City, Okinawa, Japan, 2011, Paper No. ISTS 2011-j-21s.

[5] Nishizawa, M., Ikeda, T., Ozaki, J., Tahara, H., Watanabe, Y., Enoguchi, A. and Takryama, N.," Development of a High-Resolution Camera System onboard Nano-Satellite PROITERES," 28th International Symposium on Space Technology and Science, Okinawa Convention Center, Ginowan-City, Okinawa. Japan, 2011, Paper No. ISTS 2011-n-08.

[6] Ikeda, T., Ozaki, J., Araki, S., Nishizawa, M., Inoue, Y., Iguchi, T., Tahara, H., and Watanabe, Y.," Research and Development of Nano-Satellite PROITERES Series at Osaka Institute of Technology," 28th International Symposium on Space Technology and Science" Okinawa Convention Center, Ginowan-City, Okinawa, Japan, 2011, Paper No. ISTS 2011-j-21.

[7] Ozaki, J., Ikeda, T., Araki, S., Nishizawa, M., Inoue, Y., Iguchi, T., Tahara, H. and Watanabe, Y.," Development of Nano-Satellite PROITERES with Electric Rocket Engines at Osaka Institute of Technology," 28th International Symposium on Space Technology and Science, Okinawa Convention Center, Ginowan-City, Okinawa, Japan, 2011, Paper No. ISTS 2011-b-13.

[8] Ozaki, J., Ikeda, T., Fujiwara, T., Nishizawa, M., Araki, S., Tahara, H. and Watanabe, Y.," Development of Osaka Institute of Technology Nano-Satellite "PROITERES" with Electrothermal Pulsed Plasma Thrusters," 32nd International Electric Propulsion Conference, Kurhaus, Wiesbaden, Germany , 2011, Paper No. IEPC-2011-035.

[9] Inoue, Y., Ozaki, J., Ikeda, T., Tahara, H. and Watanabe, Y.," Research and Development of Osaka Institute of Technology Nano-Satellite "PROITERES" with Electrothermal Pulsed Plasma Thrusters," Asian Joint Conference on Propulsion and Power 2012, Grand New World Hotel, Xi'an, China, 2012, Paper No. AJSPP2012-005.

[10] Egami, N., Inoue, Y., Nakano, S., Ikeda, T. and Tahara, H.," Research and Development of Nano-Satellite PROITERES with Electric Rocket Engines at Osaka Institute of Technology," 8th IEEE Vehicle Power and Propulsion Conference, Olympic Parktel, Seoul, Korea, 2012, Paper No. SS01-0298.

[11] Kamimura, T., Yamasaki, K., Egami, N., Matsuoka, T., Sakamoto, M., Inoue, Y., Ikeda, T. and Tahara, H.," Final Checking Process and Launch of the Osaka Institute of Technology 1st PROITERES Nano-Satellite Using Indian PSLV Rocket C-21," 29th International Symposium on Space Technology and Science, Nagoya Congress Center, Nagoya-City, Aichi, Japan, 2013, Paper No. ISTS 2013-f-48p.

[12] Egami, N., Matsuoka, T., Sakamoto, M., Inoue, Y., Ikeda, T. and Tahara, H.," R&D, Launch and Initial Operation of the Osaka Institute of Technology 1st PROITERES Nano-Satellite and Development of the 2nd and 3rd Satellites," 29th International Symposium on Space Technology and Science, Nagoya Congress Center, Nagoya-City, Aichi, Japan, 2013, Paper No. ISTS 2013-f-12.

[13] Egami, N., Matsuoka, T., Sakamoto, M., Inoue, Y., Ikeda T. and Tahara, H.," R&D, Launch and Initial Operation of the Osaka Institute of Technology 1st PROITERES Nano-Satellite with Electorothermal Pulsed Plasma Thrusters and Development of the 2nd satellite," 33nd International Electric Propulsion Conference, George Washington University, Washington, D.C., USA, 2013, Paper No. IEPC-2013-100.

[14] Takagi, H., Yamamoto, T., Ishii, Y. and Tahara, H.," Performance Enhancement of Electrothermal Pulsed Plasma Thrusters for Osaka Institute of Technology Electric-Rocket-Engine onboard Small Space Ship," 27th International Electric Propulsion Conference, Tsukuba, Japan, 2009, Paper No. ISTS 2009-b-16.

[15] Takagi, H., Yamamoto, T., Ishii, Y. and Tahara, H.," Performance Enhancement of Electrothermal Pulsed Plasma Thrusters for Osaka Institute of Technology Electric-Rocket-Engine onboard Small Space Ship," 31th International Electric Propulsion Conference, University of Michigan, Ann Arbor, Michigan, USA, 2009, Paper No. IEPC-2009-254.

[16] Naka, M., Tanaka, M., Tahara, H., Watanabe, Y. and Wakizono, T.," Development of Electrothermal Pulsed Plasma Thruster System Flight-Model onboard Nano-Satellite PROITERES," 28th International Symposium on Space Technology and Science" Okinawa Convention Center, Ginowan-City, Okinawa, Japan, 2011, Paper No. ISTS 2011-b-03.

[17] Naka, M., Hosotani, R., Tahara, H. and Watanabe, Y.," Development of Electrothermal Pulsed Plasma Thruster System Flight-Model for the PROITERES Satellite," 32nd International Electric Propulsion Conference, Kurhaus, Wiesbaden, Germany, 2011, Paper No. IEPC-2011-034.

[18] Kawamura, T., Fujiwara, K., Uemura, K., Muraoka, R., Chen, H., Kisaki, S., Tanaka, M., Tahara, H. and Wakizono, T.," Research and Development of Electrothermal Pulsed Plasma Thruster Systems for Osaka Institute of Technology PROITERES Nano-Satellite Series," 29th International Symposium on Space Technology and Science, Nagoya Congress Center, Nagoya-City, Aichi, Japan, 2013, Paper No. ISTS-2013-055p.

[19] Muraoka, R., Chen, H., C., Kisaki, S., Tanaka, K., Tahara, H. and Wakizono, T.," Performance Characteristics of Electrothermal Pulsed Plasma Thruster Systems onboard Osaka Institute of Technology PROITERES Nano-Satellite Series," 29th International Symposium on Space Technology and Science, Nagoya Congress Center, Nagoya-City, Aichi, Japan, 2013, Paper No. ISTS 2013-b-13.

[20] Kisaki, S., Muraoka, R., Chen, H., Tanaka, M., Egami, N., Ikeda, T., Tahara, H. and Wakizono, T.," Research and Development of Osaka Institute of Technology PROITERES Nano-Satellite Series with Electrothermal Pulsed Plasma Thruster Systems," 29th International Symposium on Space Technology and Science, Nagoya Congress Center, Nagoya-City, Aichi, Japan, 2013, Paper No. ISTS 2013-b-15.

[21] Kisaki, S., Muraoka, R., Chen, H., Tanaka, M., Tahara, H., Wakizono, T.,"Research and Development of Electrothermal Pulsed Plasma Thruster Systems onboard Osaka Institute of Technology PROITERES Nano-Satellites," 33nd International Electric Propulsion Conference, George Washington University, Washington, D.C., USA, 2013, Paper No. IEPC-2013-097.

[22] Rysanek, F. and Burton, R. L.," Performance and Heat Loss of a Coaxial Teflon Pulsed Thruster," 27th International Electric Propulsion Conference, Pasadena, California, USA, 2001, Paper No. IEPC-01-151.

[23] Burton, R. L. and Turchi, P. J.," Pulsed Plasma Thruster," Journal of Propulsion and Power, Vol.14, No.5, 1998, pp.716-735.

[24] Burton, R. L., Wilson, M. J. and Bushman, S. S.," Energy Balance and Efficiency of the Pulsed Plasma Thruster," AIAA Paper No. 98-3808, 1988.
[25] Edamitsu, T., Tahara, H. and Yoshikawa, T.: Effects of Cavity Length and Material on Performance Characteristics of a Coaxial Pulsed Plasma Thruster, 24th International Symposium on Space Technology and Science, Paper ISTS-2004-b-6, 2004.
[26] Edamitsu, T., Tahara, H. and Yoshikawa, T.," Performance Characteristics of a Coaxial Pulsed Plasma Thruster with PTFE Cavity," Proceedings of Asian Joint Conferences on Propulsion and Power 2004, 2004, pp.324-334.
[27] Edamitsu, T., Tahara, H. and Yoshikawa, T.," Performance Measurement and Flowfield Calculation of a Pulsed Plasma Thruster with a PTFE Cavity," Asian Joint Conference on Propulsion and Power 2005, Kitakyushu International Conference Center, Kitakyushu, Japan, 2005, Paper No. AJCPP2005-22083.
[28] Edamitsu, T. and Tahara, H.," Performance Measurement and Flowfield Calculation of an Electrothermal Pulsed Plasma Thruster with a Propellant Feeding Mechanism," 29th International Electric Propulsion Conference, Princeton University, Princeton, New Jersey, USA, 2005, Paper No. IEPC-05-105.
[29] Tanaka, M., Naka, M., Tahara, H. and Watanabe, Y.," Flowfield Calculation of Electrothermal Pulsed Plasma Thrusters for Nano-Satellite PROITERES," 28th International Symposium on Space Technology and Science, Okinawa Convention Center, Ginowan-City, Okinawa, Japan, 2011, Paper No. ISTS 2011-b-61p.
[30] Tahara, H., Ishii, Y., Tanaka, M., Naka, M. and Watanabe, Y.," Flowfield Calculation of Electrothermal Pulsed Plasma Thrusters for the PROITERES Satellite," 32nd International Electric Propulsion Conference, Kurhaus, Wiesbaden, Germany, 2011, Paper No. IEPC-2011-037.
[31] Tanaka, M., Kisaki, S., Ikeda, T. and Tahara, H.," Research and Development of Pulsed Plasma Thruster Systems for Nano-Satellites at Osaka Institute of Technology," 8th IEEE Vehicle Power and Propulsion Conference, Olympic Parktel, Seoul, Korea, 2012, Paper No. SS01-0300.